



# A microfluidic device for noninvasive cell electrical stimulation and extracellular field potential analysis

Liwei Ni<sup>1</sup> · Pawan KC<sup>2</sup> · Emily Mulvany<sup>2</sup> · Ge Zhang<sup>2</sup> · Jiang Zhe<sup>1</sup>

Published online: 21 February 2019  
© Springer Science+Business Media, LLC, part of Springer Nature 2019

## Abstract

We developed a device that can quickly apply versatile electrical stimulation (ES) signals to cells suspended in microfluidic channels and measure extracellular field potential simultaneously. The device could trap cells onto the surface of measurement electrodes for ES and push them to the downstream channel after ES by increasing pressure for continuous measurement. Cardiomyocytes, major functional cells in heart, together with human fibroblast cells and human umbilical vein endothelial cells, were tested with the device. Extracellular field potential signals generated from the cells were recorded. We found that under electrical stimulation, cardiomyocytes were triggered to alter their field potential, while non-excitabile cells were not triggered. Hence this device can noninvasively distinguish electrically excitable cells from electrically non-excitabile cells. Results have also shown that increased cardiomyocyte cell number led to increased magnitude and occurrence of the cell responses. This relationship could be used to detect the viable cells in a cardiac tissue. Application of variable ES signals on different cardiomyocyte clusters has shown that the application of ES clearly boosted cardiomyocytes electrical activities according to the stimulation frequency. In addition, we confirmed that the device can apply ES onto and detect the electrical responses from a mixed cell cluster; the responses from the mixed cluster is dependent on the ratio of cardiomyocytes. These results demonstrated that our device could be used as a tool to optimize ES conditions to facilitate the functional engineered cardiac tissue development.

**Keywords** Electrical stimulation · Cell analysis · Microchannel · Extracellular field potential

## 1 Introduction

The roles of electrical stimulation (ES) played on regulating cell behaviours have been gradually recognized. During the past few decades, mounting studies have shown that ES could affect cell adhesion, migration, proliferation, and secretion of extracellular matrix (Fields and Itoh 1996; Kotwal and

Schmidt 2001; Zhao 2009; Zhao et al. 2003). Recently, ES has become an attractive tool for many cardiac tissue engineering applications. The exogenous ES within the physiological range (tens to hundreds of mV/mm) (Nuccitelli 1992) has been applied to various types of stem cells including human mesenchymal stem cells, adult cardiac stem cells, embryonic stem cells and induced pluripotent stem cells, which has shown that ES can direct cardiac differentiation of these stem cells. For example, the embryoid bodies (EBs) of human induced pluripotent stem cells, when applied the acute ES (65 mV/mm or 200 mV/mm amplitude, 1 Hz frequency, 1 ms pulse width, and 5 min ES duration), has shown to promote cardiomyocyte differentiation compared to the unstimulated control group as evidenced by increased percentage of beating EBs, leading to the high expression of cardiac transcription factors (NKX2.5 and TBX5) and cardiac contractile muscle proteins (ACTC1, TNNT2, MYH7, and MYL7) (Chan et al. 2013). Similarly, by applying continuous ES (6.6 V/cm, 1 Hz, and 2 ms pulses) on human embryonic stem cell (hESCs) embryoid bodies for 4 days, Chan YC et al. showed the enhanced differentiation and maturation of hESCs into cardiomyocytes compared to unstimulated cells, as

---

Liwei Ni and Pawan KC contributed equally to this work.

**Electronic supplementary material** The online version of this article (<https://doi.org/10.1007/s10544-019-0364-2>) contains supplementary material, which is available to authorized users.

✉ Ge Zhang  
ge10@uakron.edu

✉ Jiang Zhe  
jzhe@uakron.edu

<sup>1</sup> Department of Mechanical Engineering, University of Akron, Akron, OH 44325, USA

<sup>2</sup> Department of Biomedical Engineering, University of Akron, Akron, OH 44325, USA

demonstrated by increased expression of cardiac-specific genes (MLC2V, GATA4, Cardiac troponin T) and improved calcium handling of hESC-derived cardiomyocytes (Hernández et al. 2016). Studies have also suggested that ES of stem cell-derived cardiomyocytes in three-dimensional culture promoted cardiomyocyte maturation and their functional assembly into contractile engineered cardiac tissues (Eng et al. 2016). These reports have suggested the functional benefits of ES for biomedical applications.

To study the influences of ES on cells, multiple approaches have been developed to apply ES to cells *in vitro*, including chamber, micro electrodes array (MEA), and microfluidic based methods. In chamber-based extracellular ES methods, cells are cultured in a chamber (either a common cell culture dish or a custom-made polydimethylsiloxane (PDMS) container) and then stimulated by electrical signals such as sine waves, square waves or pulses (Serena et al. 2009)(Du et al. 2016; Kim et al. 2006; Lluçia-Valldeperas et al. 2015; Lluçia-Valldeperas et al. 2014; Pavesi et al. 2014; Yuan et al. 2015). Electrical field is typically introduced into the cells cultured in the chamber by rod or planar electrodes that are submerged in the culture medium. This approach uses devices that are easy to fabricate and can directly apply ES to a large number of cells. However, the approach is designed for characterizing biological behaviours of cells (viability, proliferation, migration, etc.). In general, it is unable to record the responsive electrical signals from the stimulated cells, which is critical to elucidate the relationship between ES and cell responses.

To be able to not only apply ES signals on cells but also measure the responsive electrical signals of cells, micro electrodes array (MEA) based stimulation (Al Abed et al. 2015; Ahadian et al. 2012; Cheng et al. 2010; Klauke et al. 2003) and recording (Blanche 2005; Dai et al. 2016; Eytan and Marom 2006; Heer et al. 2005; Hutzler 2006; Huys et al. 2012; Jenkner et al. 2004; Joucla and Yvert 2012; Jun et al. 2007; Spira and Hai 2013) methods have been developed (Martinoia et al. 2001; Stett et al. 2003). The use of MEA method has increased the signal strength and resulted in a better signal-to-noise ratio (SNR), which can provide details about cell field potential (FP) and also be utilized in long-term pacing experiments (Frey et al. 2009; Huys et al. 2012; Klauke et al. 2003). Still, this method requires the precise and firm attachment of testing cells onto the array of electrode for accurate ES and recording (Ahadian et al. 2012; Jun et al. 2007). However, the precise placement of cells on MEA has been known to be challenging and time consuming (Klauke et al. 2003).

Recently, microfluidics based ES methods have been explored to electrically stimulate cell clusters or single cells without the need for attaching/growing cells on the electrodes, and were often combined with MEA to achieve simultaneous stimulation and response recording (Cheng et al. 2006; Klauke et al. 2006; Myers et al. 2013; Myers et al. 2011; Wu et al. 2015). Cheng et al. fabricated a micro chamber with

embedded microelectrodes to apply ES on single cells and measure the cell responses, which still required manually positioning the cells onto the microelectrode surface by micropipette (Cheng et al. 2006). Myers et al. invented a microfluidic device with microelectrode arrays, which positioned individual cell clusters onto the electrode surface by stopping the flow once a cell cluster was detected (Myers et al. 2011)(Myers et al. 2013). However, it is difficult to locate each cell cluster onto the same position due to the inertia movement. As the measured signal (the cell cluster's extracellular field potential) is dependent on the distance from cell cluster to the measurement electrodes, the uncertainty caused by cell position may create measurement errors. Similarly, in the device reported by Klauke et al., a barrier dam was used to stop one single cell in a micro cavity with embedded measurement microelectrodes (Klauke et al. 2006). However, after the electrical stimulation/measurement, the cell cluster must be taken out from the micro chamber/channel in order to apply ES on the next cell cluster; the whole procedure was lengthy and low throughput.

Here, we report a microfluidic device that can quickly apply versatile ES signals to cells and record cell electrical responses simultaneously within minutes. By controlling the driving pressure of the flow and using a constriction channel, a cell cluster can be easily located onto the surface of measurement electrodes for ES and be driven to the downstream channel after ES such that the next cluster can be electrically stimulated and measured in a continuous flow. Hence the device enables continuous application of ES to individual cell cluster and measurement of cluster's responses with higher throughput. To validate our device, ES was applied to clusters consisting of three different types of cells, including human cardiac myocytes (hCMs), human fibroblast cells (hDFs), and human umbilical vein endothelial cells (hUVECs). Electrical responses of these cell clusters were recorded. Next, the effect of human cardiac myocyte cluster size, frequencies of ES, and mixed cell populations on cell electrical responses were investigated.

## 2 Materials and methods

### 2.1 Materials

Human cardiac myocytes (electrically excitable cells), myocyte growth medium kit, detach kit, and cryo-SFM were purchased from PromoCell GmbH (Heidelberg, Germany). Human dermal fibroblasts and human umbilical vein endothelial cells (electrically non-excitable cells), and EGM-2 Bulletkit were purchased from Lonza (Walkersville, MD, USA). Trypsin/EDTA, fetal bovine serum, and antibiotic-antimycotic solutions were obtained from Gibco (Carlsbad, CA, USA). Dulbecco's modified eagle's medium and cell culture grade 1X phosphate buffered saline solution were

obtained from Corning (Manassas, VA, USA). Trypan Blue (0.4%) solution was obtained from ScienceCell Research Laboratories (Carlsbad, CA, USA). AggreWell™ 800 24-well plate and anti-adherence rinsing solution were purchased from StemCell Technologies (Vancouver, BC, Canada). Silicone elastomer kit was purchased from Dow Corning (Copley, OH, USA). Gold coated glass slides were purchased from Dynasil (Newton, MA, USA). All materials were used as received from the manufacturer.

## 2.2 Device design

The device for cell electrical stimulation was designed to quantitatively measure responses from cell clusters (Fig. 1). The device consists of 1) an inlet reservoir with a 1.5 mm diameter access hole for loading the cell cluster, 2) a 500  $\mu\text{m}$  wide main fluidic channel, 3) a constriction microchannel with dimensions of 100  $\mu\text{m}$  (height)  $\times$  30  $\mu\text{m}$  (width)  $\times$  50  $\mu\text{m}$  (length) between the pair of the measurement electrodes to trap and locate the cell cluster on top of the left measurement electrode, 4) a pair of 500  $\mu\text{m}$  wide stimulation electrodes for applying electrical

stimulation signals, 5) a pair of 100  $\mu\text{m}$  wide measurement electrodes located in both sides of the constriction channel for measuring the extracellular field potential, and 6) an outlet reservoir with a 1.5 mm diameter access hole to collect the cell clusters after electrical stimulation.

## 2.3 Device fabrication

The standard soft lithography process was used to fabricate the device. First, a SU8 (2025, MicroChem) master mold, consisting of patterns for microchannels, fluidic chamber, inlet and outlet reservoirs, was created using photolithography. Second, a gold-coated glass slide (1"  $\times$  3", EMF Corporation) with 100 nm/10 nm gold/titanium coating was used to fabricate the microelectrodes. Standard lithography followed by wet etching with KI/I2 gold etchant (Sigma-Aldrich) was applied to the glass slide to pattern the measurement electrodes and stimulation electrode. Third, the microchannel was bonded to the glass slide after an oxygen plasma treatment (200 mTorr, 50 W, 50 s). The dimensions of the constriction microchannel measured by the surface profilometer (Dektak

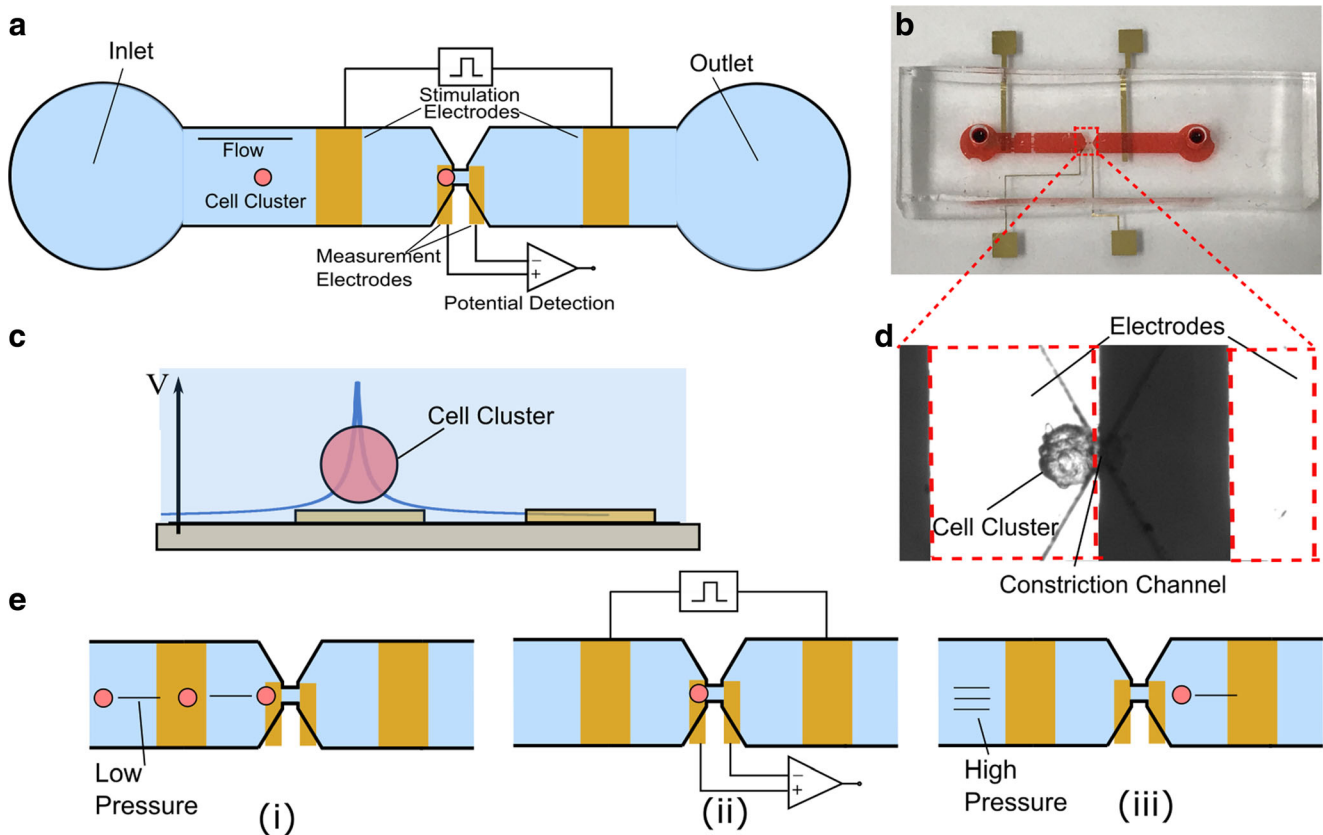


**Fig. 1** Schematic diagram of the sensing principle of the electrical stimulation system. **a** Illustration of the stimulation and measurement of cell clusters. **b** Picture of the electrical stimulation device. **c** Cross-sectional view and illustration of the resulted extracellular field potential (FP) signal in the surrounding resistive medium of a cell.  $V$  is the local electric potential. **d** Microscopic photo of a cell cluster trapped onto the measurement electrode. **e** Stimulation and

measurement process: i) the cell cluster was loaded from the inlet and trapped on top of the measurement electrodes using low pressure flow. ii) The electrical stimulation was applied and the response of each cell cluster was measured. iii) After the measurement, the cell cluster was pushed downstream through the constriction microchannel using a high pressure flow

150, Veeco Instrument) were  $47.58 \mu\text{m} \pm 0.87$  (length),  $98.24 \pm 2.45 \mu\text{m}$  (depth), and  $31.54 \pm 1.51 \mu\text{m}$  (width).

## 2.4 Cell culture

Human cardiac myocytes (hCMs; C-12810) were cultured in myocyte growth medium kit following the manufacturer's instruction. According to the manufacturer, these cells were isolated from normal human ventricle tissue of the adult heart but act more like 'progenitor' cells in that they are not fully differentiated. Because their immature status, these cells cannot be induced to contract or beat. Human umbilical vein endothelial cells (hUVECs) were cultured in EGM-2 bulletkit, supplemented with 1% antibiotic-antimycotic solution. Human dermal fibroblasts (hDFs) were maintained in a Dulbecco's modified eagle's medium (DMEM), supplemented with 10% fetal bovine serum and 1% antibiotic-antimycotic solution. Cells were maintained in a humidified cell culture incubator at  $37^\circ\text{C}$  and 5%  $\text{CO}_2$  with respective growth medium. Cell culture medium was changed every other day for hCMs and every 2 days for hUVECs and hDFs. Once the cells reached 80–90% confluence, they were sub-cultured using PromoCell detach kit for hCMs and 0.25% Trypsin/EDTA solution for hUVECs and hDFs. All experiments were performed using hCMs at passages 6–9, hDFs at passages 9–11, and hUVECs at passages 10–12.

## 2.5 Cluster formation and harvesting

Cells were aggregated to form cell spheroids using AggreWell 24-well plate following the manufacturers' recommendation. Briefly, each well of AggreWell plate was incubated with 500  $\mu\text{L}$  of anti-adherence rinsing solution at room temperature for 15 min. After the incubation, the plate was centrifuged at  $2000 \times g$  for 5 min in a swinging bucket rotor fitted with plate holders. The anti-adherence rinsing solution was discarded from the wells and washed once with 1 mL of complete cell growth medium. Next,  $15 \times 10^3$  and  $25 \times 10^3$  cells were seeded on the AggreWell plate maintaining the final volume of respective cell culture medium to be 1 mL on each well. For mixed cell population samples, hCMs and hUVECs were seeded at the ratio of 1:1 and 1:2 using the culture medium containing equal ratio of cardiac myocyte growth medium and EGM-2 growth medium. The total number of cells was maintained to be  $25 \times 10^3$  for the mixed cell population samples. Immediately after cell seeding, the cells were mixed with a pipette to ensure even distribution of cells throughout the well and centrifuged at  $100 \times g$  for 3 min to capture cells in the microwells. The cells were incubated in a humidified cell culture incubator ( $37^\circ\text{C}$ ; 5%  $\text{CO}_2$ ) for 48 h before collecting the cell clusters for experiments. For harvesting the cell clusters, the tip of the 1000  $\mu\text{L}$  pipette tip was cut using sterile scissor inside the cell culture hood. The cell clusters were then

dislodged by pipetting up and down several times before collecting the cell clusters suspension. After collecting the suspension, the tube containing the cells was incubated vertically at room temperature for 10 min to let the cell clusters sediment on the bottom of the tube. To obtain desired cell cluster concentration, the appropriate volume of cell culture medium was aspirated from the top of the tube using 1000  $\mu\text{L}$  pipette. The concentration of each sample was maintained to be 600 clusters per mL. All samples were prepared with 3–6 independent replicates.

## 2.6 Cell cluster analysis

Phase contrast images of cell clusters were captured using an inverted AxioVision A1 microscope (Carl Zeiss, Oberkochen, Germany). The nominal diameter of the clusters was quantitatively measured using an ImageJ image processing software (National Institutes of Health). For each cluster sample, the horizontal and vertical diameters were measured and averaged to represent the diameter of the cluster, and average number of 20 representative clusters' diameters were taken to quantify the average size of cell clusters within the well. The approximate cell number in the cell clusters were calculated based on the total number of the seeded cells and the number of the formed cell clusters. To form cell clusters, we seeded  $15 \times 10^3$  (for small size cluster) and  $25 \times 10^3$  (for large size cluster) cells to each well of the commercially available AggreWell™ 24-well plate. Following the manufacturer's protocol, each well produced ~300 uniform cell clusters. By dividing the total cell number seeded in each well of the plate with cell cluster number (~300), we obtained the average cell number of ~50 cells/cluster for small size cluster and 83 cells/cluster for large size cluster.

## 2.7 Operation procedures and sensing principle of electrical stimulation system

Cell clusters were loaded into the device at a concentration of 600 cell clusters per mL. A constant pressure of 3 kPa was applied through the inlet reservoir using a flow controller (Flow-EZ, Fluigent, France) to control the flow. A constriction microchannel between the pair of the measurement electrodes was used to trap and locate the cell cluster on top of the left measurement electrode. Cell clusters with sizes from 40  $\mu\text{m}$  to 100  $\mu\text{m}$  can be held on the electrodes according to the dimensions, which was verified by experiments. Clusters out of this size range can be tested by changing the channel dimensions.

When the cell cluster was trapped on the measurement electrode surface, the flow velocity was approximately zero since the constriction channel was nearly blocked by the cluster. Once the cell trap was confirmed by observation from the microscope, the pressure was removed by turning off the flow controller; ES was then applied to the cell cluster and FP was recorded. Due to the low concentration, each time only one



cluster was trapped. The cluster was located and immobilized on the surface of the detection electrodes (Fig. 1a, d). Next, the exertion and detection of electrical signals from the cell cluster were carried out by two pairs of co-planar gold electrodes. The wide electrodes (stimulation electrodes) were used to apply the electrical stimulation. The cells contain highly conductive aqueous electrolytes separated by thin, low-conductivity membranes, and populated with electrically active macromolecules. The electrical responses of cells to ES depend on the ES-induced cell membrane alterations such as the status changes of ion pumps voltage-gated channels, electroporatable membrane regions. Therefore, when a cell is excited by ES to trigger cell membrane alterations, the resulting extracellular field potential change (cell responses) could be quantitatively recorded using the pair of the measurement electrodes. Note that the magnitude of the field potential is inversely proportional to the distance from the cell, which means that the field potential drops dramatically when distance between the cell and the electrode increases (Kim et al. 2006) (Fig. 1b). As a result, the device only detects the field potential signal from a single cluster when there is only one cluster held on the electrodes, while field potentials from other clusters away from the electrodes cannot be detected.

## 2.8 Measurement setup

The device was positioned under an upright microscope (PSM-1000, Motic) equipped with a video camera (QICAM 12-bit, QIMAGING) for visual inspection of cell positioning. The entire system was enclosed in a custom-made Faraday cage with dimensions of 0.6 m(length)  $\times$  0.6 m(width)  $\times$  0.5 m(height) to minimize radio frequency and power line interferences. The Faraday cage was made of 1.5 mm thick aluminum alloy sheets. Excitation signals were generated from a waveform generator (33600A, KEYSIGHT) and applied on the microfluidic channel through the stimulation electrodes. Here we used current stimulation signals instead of voltage stimulations because the current stimulation can ensure the cell clusters received uniform electrical stimulation (Schuettler et al. 2008). According to the work of Klauke et al. (Klauke et al. 2003), a stimulation electrical field larger than 40 V/cm would cause electrolysis and irreversible damage to the cells. The maximum electrical field used in our experiments was 5.6 V/cm, which was much smaller than that threshold. Custom LabVIEW software connected to a data acquisition board (PCI-6133, National Instrument, USA) was used to record and digitize signals from the device at a sampling rate of 1.5 MHz.

## 2.9 Stimulus artifact elimination and signal processing

Because the field potential signals from a cell cluster are much smaller than the stimulation signals, the measured signals

were processed with both hardware and software methods. Measurement circuit along with signal processing algorithm were applied on the output signals from the measurement electrodes to reduce the capacitive coupling of the stimulus and detection electrodes. The circuit used a FET-input instrumentation amplifier (Instrumentation Amplifier AD8220ARMZ, Analog Devices Inc., USA), a monolithic sample-and-hold circuit (LF298 Monolithic Sample-and-Hold Circuits, Texas Instruments Inc., USA) and a two-stage op-amp bandpass filter with a passband of 4 Hz – 50 kHz. The whole gain for the amplifier and filter was 1000. Details of the circuit are shown in supporting materials. Software bandpass filters were also used to further eliminate the stimulus signals and increase the signal-to-noise rate.

## 2.10 Cell viability

The viability test of hCM cluster before and after ES was performed using LIVE/DEAD viability/cytotoxicity kit (ThermoFisher Scientific, Waltham, MA, USA) following the manufacturer's recommendation. Briefly,  $25 \times 10^3$  hCMs were seeded on each well of AggreWell 24-well plate and incubated at humidified cell culture incubator (37 °C; 5% CO<sub>2</sub>) for 48 h. After incubation, the cell cluster was harvested and stained with calcein-AM (1  $\mu$ M) for live cells, ethidium homodimer (4  $\mu$ M) for dead cells, and hoechst (1:1000) for cell nuclei. For no ES experiment group, the cell clusters were passed through the microfluidic device driven by a constant pressure of 3 kPa without applying ES. For ES experiment group, the cell clusters were forced to pass through the device under the same pressure and applied the ES (0.4 mA; 2 Hz pulses with a 0.5 ms pulse width for 60 s interval). The cell cluster before passing through the microfluidic device was used as controls for each tested group. Z-stack images of cell cluster were taken using a FluoView FV1000 confocal microscope (Olympus, Center Valley, PA, USA). The cell viability percentage was quantified using ImageJ software (NIH free software) based on the pixel intensities of green (calcein-AM) and red (EthD-1) fluorescence signals as previously described (Chambers et al. 2014). Student's *t* test was used to determine the statistical significance difference between the samples before and after cell analysis.

## 2.11 Statistical analysis

The results are presented in means  $\pm$  standard deviation (SD) with 3–6 independent samples. We performed statistical analysis using the Graphpad Prism 5 software (La Jolla, Ca, USA). Student's *t* test was performed for comparing the significant difference between two experimental groups. Analysis of variance (ANOVA) and Tukey's post hoc test was used to compare the differences among three or more experiment groups. A *p* value of less than 0.05 was considered to be statistically significant.

### 3 Results

#### 3.1 Device validation using non-excitabile and excitable cells

The baseline signal of our device was first obtained by measuring the field potential between the two measurement electrodes without the presence of cell cluster and input signals (Fig. 2a). The range of the baseline signal was found to be between  $-3 \mu\text{V}$  to  $3 \mu\text{V}$ , which was possibly caused by the noises from the measurement circuit. Next, cell clusters consisting of same cell number ( $\sim 83$  cells per cluster) were formed using electrically non-excitabile cells (hDFs: human fibroblast cells; hUVECs: human umbilical vein endothelial cells) and electrically excitable cells (hCMs; human cardiac myocytes) separately. Cell clusters were loaded into our device and positioned onto the stimulation electrode surface. Figure 2a indicated that without input electrical signal, the presence of non-excitabile cell clusters did not alter the baseline signal. The cell clusters then underwent electrical stimulation. The caused fluctuations of field potential were recorded by the measurement electrodes. (See Fig. 2b) When the electrical stimulation signals (0.4 mA, 0.5 Hz pulses with a 0.5 ms pulse width, 60s) were continuously applied, the electrical activities of the cell cluster made of human cardiac myocytes (electrically excitable cells) were triggered; clearly identified waveform patterns were detected with the peak value ranging from  $-30 \mu\text{V}$  to  $15 \mu\text{V}$ . However, under the same electrical

stimulation condition, no significant difference was found between the responses from hDF cluster (or hUVEC cluster, both are electrically non-excitabile cells) and the baseline signals. This indicates non-excitabile cells did not respond to the ES input. Hence from the cell responses, we can distinguish electrically excitable cells from the electrically non-excitabile cells. Spontaneous electrical activities of hCMs were also observed before ES. However, during the stimulation, cell responses from hCMs showed an increase in both magnitude and occurrence rate compared to the spontaneous responses. Details are discussed in Section “Cell Electrical Responses Before, during and After ES”. The ES parameters used here were based on published results from other research groups (Myers et al. 2011)(Myers et al. 2013). It needs to be noted that although we only showed results under one ES signal (0.4mA, 0.5 Hz pulse), we applied various ES signals with different frequencies and magnitudes to the cell clusters. While we did not detect any electrical response from the non-excitabile cells (hDFs and hUVECs), we did observe that the excitable cells (hCMs) responded differently to different ES signals. The excitable cells (hCMs) were observed to respond differently to ES signals with different frequencies (see details in Section “The Effect of ES Frequency on hCM Cluster Responses” and Fig. 6). ES signals with different magnitudes (0.1–0.8 mA) were also applied to hCM clusters. When the ES magnitude was between 0.1 and 0.3 mA, the clusters’ FP signals (magnitude and occurrence) did not show detectable difference compared to those of spontaneous

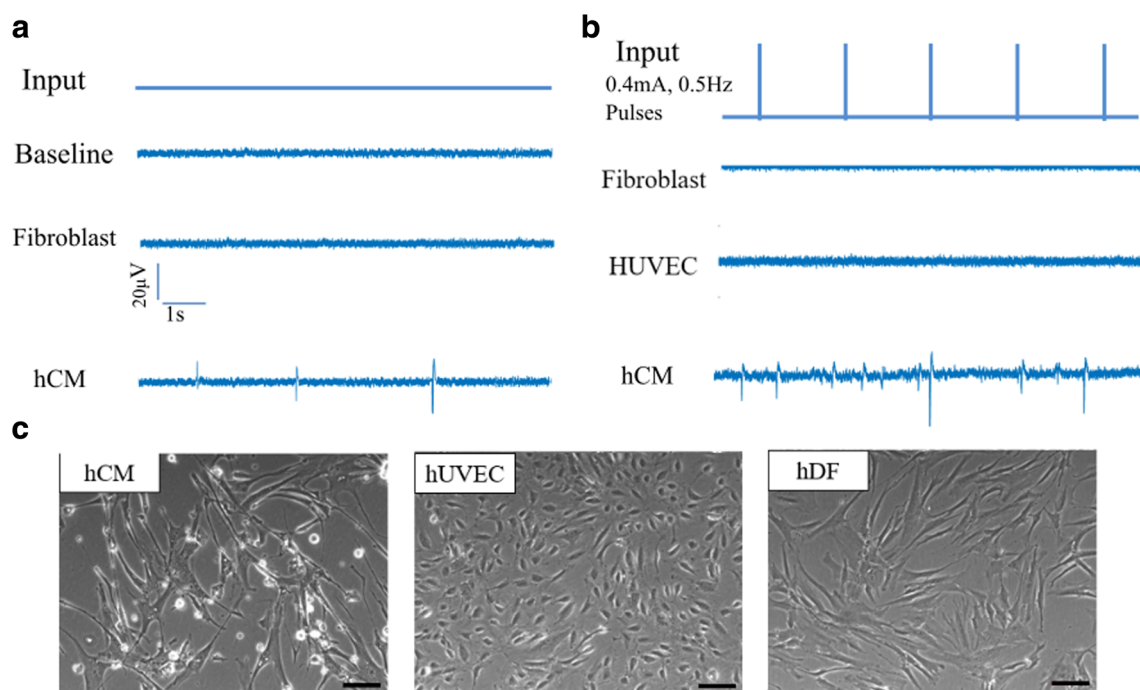


**Fig. 2** Device validation using 3 types of cells. **a** Detected field potential signals from the device without input signals. **b** Detected response signals from cell clusters made of 3 types of cells when stimulated using the same

input signals (0.4 mA, 0.5 Hz pulses with a 0.5 ms pulse width, 60s). **c** Representative phase contrast images of the 3 types of testing cells (hDFs, hUVECs and hCM). Scale bar 100  $\mu\text{m}$

electrical activities. When the stimulation magnitude reached 0.3 mA, significant increase in magnitude and occurrence of cell clusters' FP signals were observed. However, further increasing stimulation current from 0.3 mA to 0.8 mA did not induce additional increase in magnitude and occurrence of FP signals from cell clusters. Hence we selected 0.4 mA as the ES magnitude in subsequent studies for different cell clusters and under different frequencies.

### 3.2 Cell viability

The cell viability was conducted to determine whether the ES would cause significant cell death during the analysis. Our results showed that the ES conditions we used in this study did not cause significant cell death after cell analysis (Fig. 3). The percentage of viable cell clusters in the experiment group (without applying ES) before and after cell clusters passing through the device was  $83.32 \pm 6.30\%$  and  $82.88 \pm 5.52\%$  respectively. The viability of clusters was not significantly different after ES study ( $77.78 \pm 4.76\%$ ) compared to the control group ( $81.52 \pm 3.74\%$ ). The average time from cell harvesting to complete ES analysis was  $\sim 2$  h, indicating the feasibility of our developed device to apply ES up to 2 h without compromising the cell viability.

### 3.3 The effects of cell cluster size on cell responses

Two different sizes of hCM clusters were formed by varying the containing cell numbers (Fig. 4a). The small cluster consisted of 50 cells per cluster on average with the diameter of  $63.38 \pm 8.16 \mu\text{m}$ . The large clusters consisted of 83 cells on

average with the diameter of  $81.13 \pm 8.16 \mu\text{m}$ . Different sized hCM clusters were injected into the device and experienced the same ES (0.4 mA, 0.5 Hz pulses with a 0.5 ms pulse width, 60s). The resulted fluctuations of field potential (the cell responses) were recorded (Fig. 4c). The results demonstrated that regardless of cluster size, cell electrical responses were triggered on all clusters. The pattern of evoked field potential signals was further analyzed and compared in terms of cluster sizes (Fig. 4d, e). When a cluster was evoked, the invoked field potential of the cell cluster underwent a rapid drop, then raised above 0 V and finally returned to baseline. The magnitude change in the stimulated field potential was measured using the peak-peak voltage (highest potential minus lowest potential) of each potential pulse signal. The occurrence of the cell responses is the average number of the identified field potential pulses per second during the ES period. A trend of increased magnitude and occurrence with the increased cluster size was observed. Significant differences in magnitude and occurrence of the cell responses were found between the different size clusters. Since the measured signals were the collecting electrical response from all hCMs excited by the ES in the clusters, the results demonstrated that under the same ES conditions, the clusters consisting more hCMs had increased electrical activities triggered by ES.

### 3.4 Cell electrical responses before, during and after ES

Similar patterns of the electrical responses were observed from differently sized hCM clusters before, during and after ES (0.4 mA, 0.5 Hz pulses with a 0.5 ms pulse width, 60s)

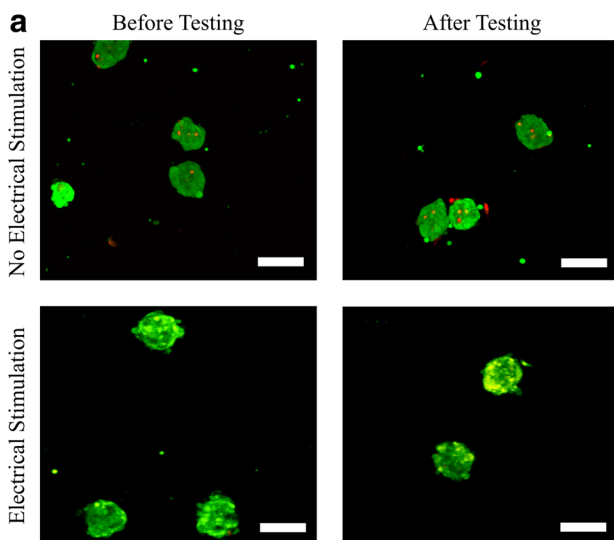
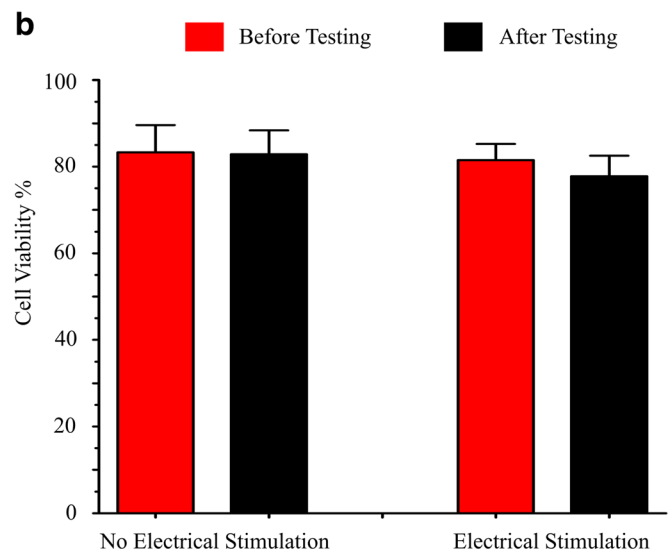


**Fig. 3** Cell viability of hCM clusters before and after the ES. **a** Z-stack confocal images of hCM clusters stained with calcein-AM (green) and ethidium homodimer-1 (red) before and after testing for experiment groups with ES and without ES, **b** Percentage of viable cells within the



cell cluster. The fluorescence intensities of green and red signals were used to calculate the cell viability. Student's t test showed no statistically significant difference between the tested groups. Scale bar  $100 \mu\text{m}$

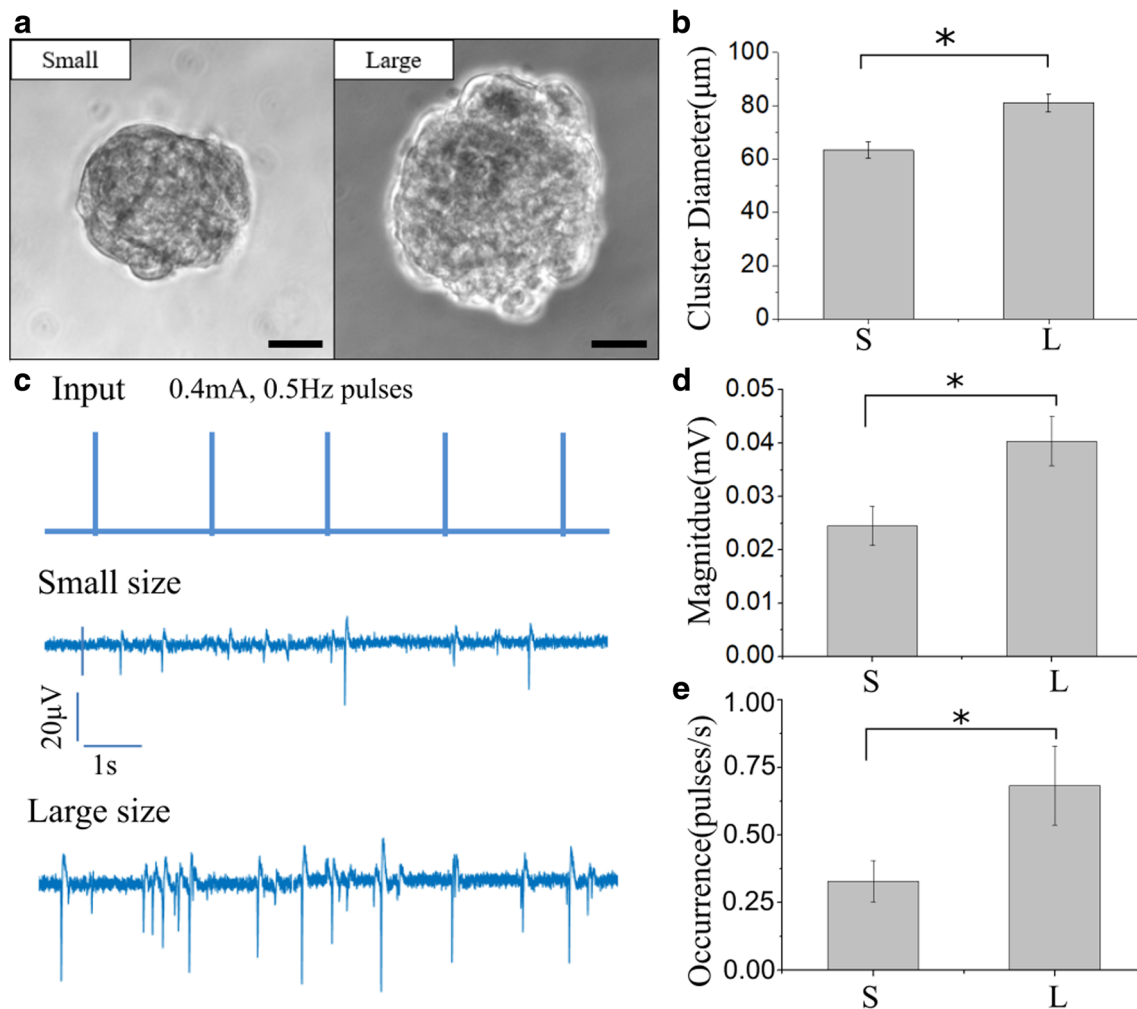


**Fig. 4** Measured cell responses from different sized hCM clusters. **a** Representative images of cell cluster with small (~50 cells/cluster) and large size (~83 cells/cluster). **b** Diameters of different clusters. **c** Typical field potential pulses generated during electrical stimulation by different size hCM clusters. **d** The quantification of average magnitude and **e**

Occurrence of response signals measured during the electrical stimulation of hCMs. \* represents statistically significant difference between the two experiment groups with  $p$  value less than 0.05. Scale bar 25  $\mu\text{m}$

(Fig. 5a). Before ES, cell responses showed a similar level of spontaneous electrical activity of hCMs. ES significantly increased both the magnitude and the occurrence of the responsive field potential pulses compared with those before and after ES. When further analyzing the average magnitude and occurrence number of each 10 s period during a 60 s electrical stimulation, the peak values of both magnitude and occurrence of large size hCM clusters appeared earlier than that generated from small size hCM clusters. This trend was repetitively observed from multiple tests. The peak values of electrical response signals suggested the synergy of electrical activities among cells. Compared with smaller size cell cluster, the earlier appearance of peak responses from the larger size cell cluster has indicated enhanced cell electrical response to the applied ES. The possible cause could be that a large size cluster contains more excitable cells that would enhance local heterogeneities and action potential generation. Transient

increasing of cell cluster electrical activity has been observed during ES. Similar trend has been reported by other groups when applying ES on cardiomyocytes (Cheng et al. 2006; Klauke et al. 2003). These studies have suggested that ES may alter the metabolic status of the stimulated cells, which would lead to local accumulation of metabolic products (e.g. acid) and therefore affects cell contractility and action potential generation.

### 3.5 The effects of ES frequency on hCM cluster responses

Large hCM clusters with the diameter of  $81.13 \pm 8.16 \mu\text{m}$  were subjected to ES (0.4 mA pulses with a 0.5 ms pulse width, 60s) at various frequencies (0.5 Hz, 1 Hz and 2 Hz) and their electrical responses were recorded and compared (Fig. 6). The results showed that the alteration of ES



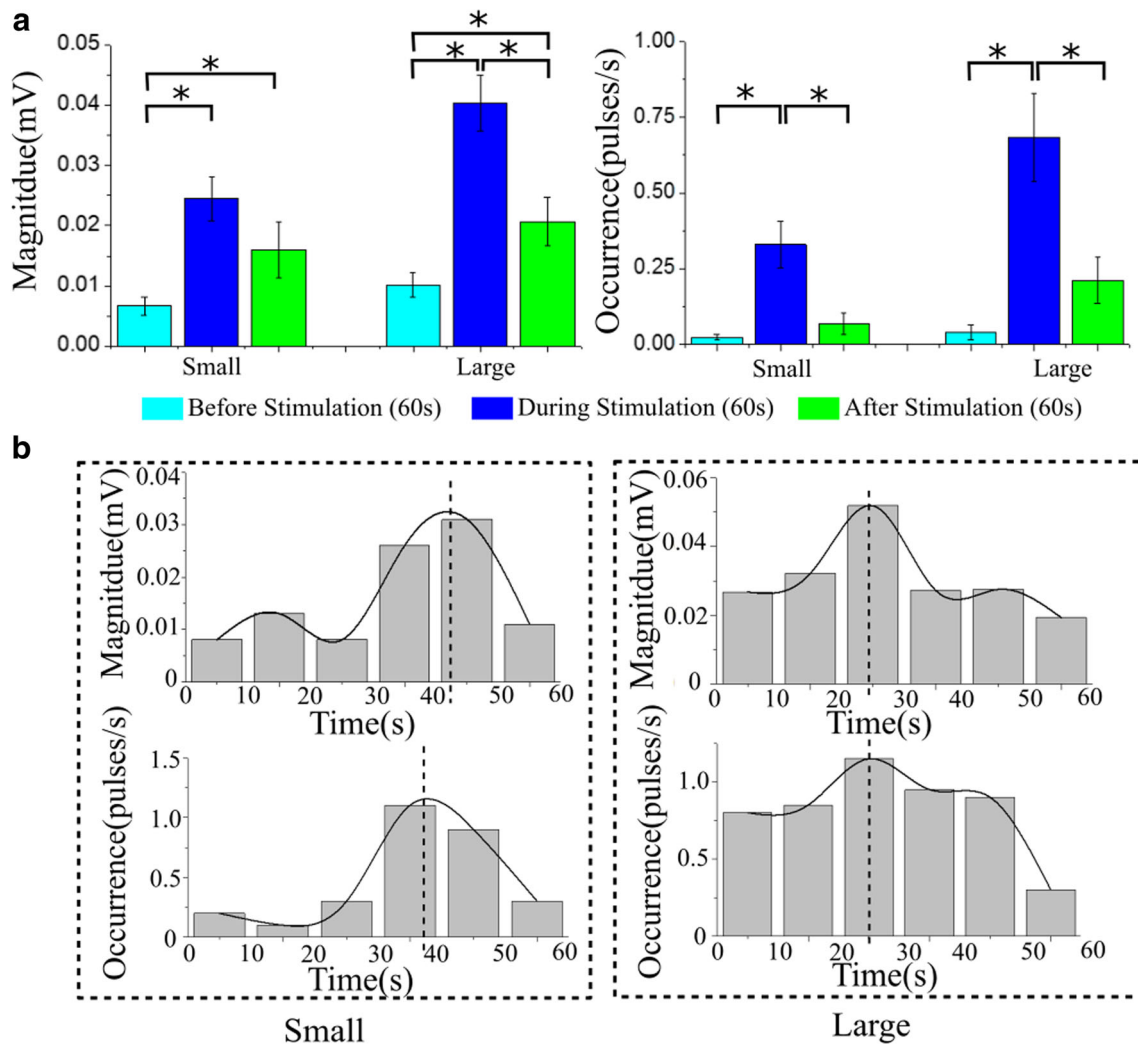


**Fig. 5** Measured responses before, during, and after the ES of cells. **a** The average magnitude and occurrence of cell responses before, during, and after ES by different size of hCM clusters. **b** Histogram distribution of

occurrence and magnitude responses by hCM clusters of varying sizes. \* represents statistically significant difference between the two experiment groups with  $p$  value less than 0.05

frequencies from 0.5 Hz to 2 Hz did not significantly change the average magnitude of field potential pulses. However, the occurrence of the cell response signals during ES period significantly increased from 13.65 (under 0.5 Hz ES) to 25.75 (under 2 Hz ES) on average. Our results showed that frequency of ES played important role in triggering hCMs electrical responses. Higher frequency ES triggered more cell electrical activities in the cell cluster. The obtained information could be used to optimize the design of future bioreactors to apply specific ES to cardiac tissue construct to achieve the desired electrical properties.

### 3.6 The effects of cell types on detecting signals

To simulate the cell composition in real heart, mixed cell clusters with the diameter of  $81.13 \pm 8.16 \mu\text{m}$  were formed using both of the electrically excitable cells (hCMs) and electrically non-excitable cells (hUVECs) at the ratio of 1:1 and 1:2. These

mixed cell clusters were electrically stimulated (0.4 mA, 1 Hz pulses with a 0.5 ms pulse width, 60s) and their responses were obtained using the device. The results are shown in Fig. 7. Although ES triggered electrical response of all the tested cell clusters, the incorporation of non-excitable hUVECs in the cell cluster significantly reduced the magnitude of the detecting signals. Moreover, the occurrence of cell responses was significantly reduced for the mixed cell cluster with the 1:2 cell ratio (hCMs to hUVECs) compared to all the mixed cell clusters with the mixed ratio of 1:1. The reduced excitable cell number and interrupted cell-cell contact among excitable cells were thought to be the main causes of the decreased electrical responses in the mixed cell clusters. Most engineered cardiac tissue constructs contain multiple cell types including cardiomyocytes. Our results indicated that this device has potentials to be used for non-invasive measurement of the ratio of functional cells (cardiomyocytes) and electrical properties of engineered cardiac tissue construct.

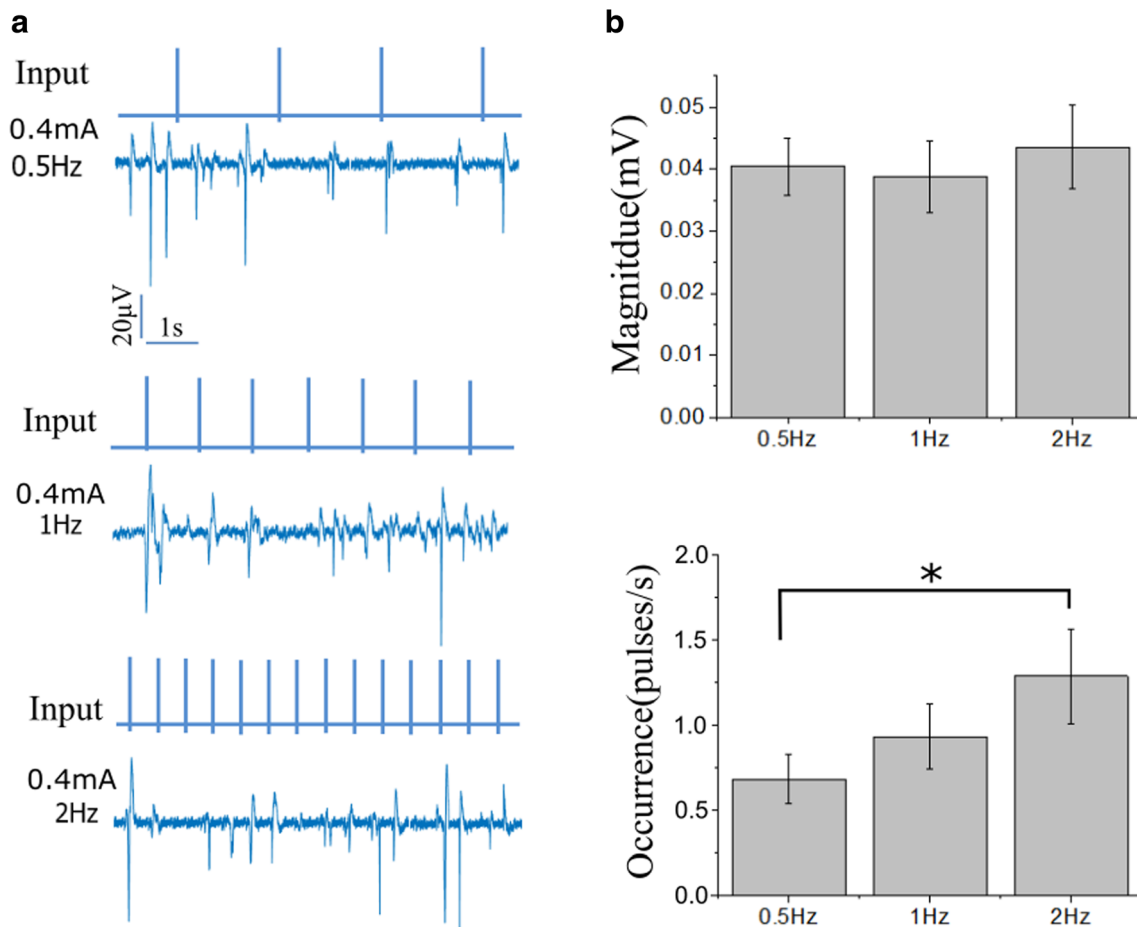


**Fig. 6** Effect of stimulation frequencies on responses of hCM clusters. **a** The cell response signals measured from hCMs at 0.5 Hz, 1 Hz, and 2 Hz. **b** The magnitude and occurrence of response from hCM clusters at

0.5 Hz, 1 Hz, and 2 Hz. \* represents statistically significant difference among the experiment groups with  $p$  value less than 0.05

## 4 Discussion

We developed a simple microfluidic chip device that can not only apply versatile ES signals to cells but also enable the measurement of cell electrical responses (extracellular field potential). With the constriction microfluidic channel and controlled pressure flow, cell clusters could be positioned on the surface of an electrode and be stimulated under variable ES signals. The changes in field potentials could be measured simultaneously. Each time after a cell cluster was stimulated and measured, the cluster could be driven to downstream for subsequent characterization and be collected at the outlet for other applications. Compared to other cell electrical stimulation method, microfluidic-based ES approach does not need to grow or attached cells on a surface, which allows cell manipulation and rapid measurement. Additional functions including cell count, size measurement and cell cycle analysis can be integrated into the device for subsequent cell characterizations after the cells are electrically stimulated.

We demonstrated some potential biological applications of our device. We found that electrically excitable cells could be

triggered to alter their field potentials, which was reflected as a clear waveform in the measured signals. Therefore, this device can noninvasively distinguish electrically excitable cells from electrically non-excitable cells, and potentially be used for cell sorting. Tests also demonstrated the relationship between cell number and detecting signals under same ES conditions. Increased cell number was associated with increased magnitude and occurrence of the cell responses. This relationship could be used to detect the viable cells in a cardiac tissue or tissue construct. Our results demonstrated that the application of ES clearly boosted cardiomyocytes electrical activities, as evidenced by increased magnitude and occurrence of field potential pulses. In addition, the level of the triggered electrical activities can be regulated by the frequency of the ES. In human heart, other than cardiomyocytes, there are other types of cells such as endothelial, fibroblast and smooth muscle cells. By testing the device using clusters containing different ratios of cardiomyocytes and non-cardiomyocytes cells, we confirmed that the device can apply ES onto and most importantly detect the electrical responses from a mixed cell population. Note this device is designed to stimulate cells with

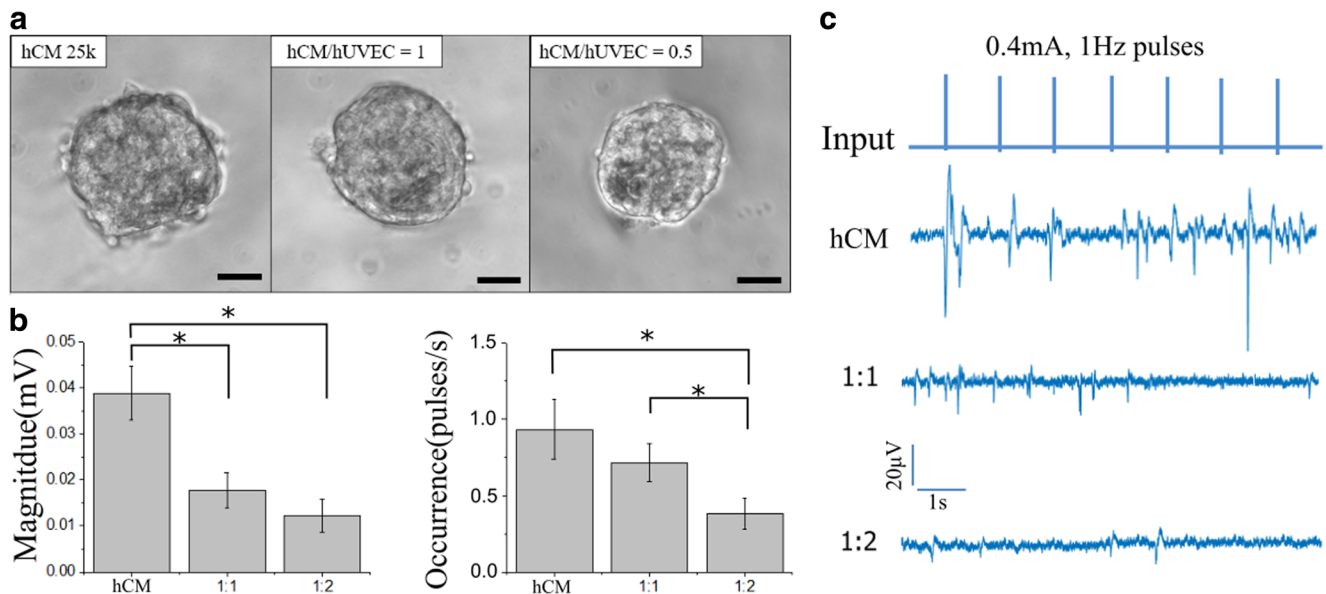


**Fig. 7** Measured cell response invoked by electrical stimulation from mixed cell clusters. **a** Phase contrast images and typical pulse generated during the electrical stimulation by the mixed population of hUVECs and hCMs at the ratio of 1:1 and 2:1. **b** The quantitative measurement of

magnitude and occurrence of cell response by the mixed cell population. \* represents statistically significant difference between the two experiment groups with  $p$  value less than 0.05. Scale bar 25  $\mu$

frequencies at physiological range (under 5 Hz). Platinized electrodes can be used to further increase the operating frequency range of this device (Malleo et al. 2010). It needs to be noted that commercial available human cardiac myocytes were used in this study, which were harvested from fresh human ventricular tissue and highly express immature cardiac progenitor markers. These cells were not able to be chemically or electrically induced to spontaneous beating and had inconsistently electrical response to a given electrical stimulation according to the manufacturer (PromoCell) as well as our preliminary studies. In addition, within the cell clusters, cell-cell electrical coupling varied depending on the local cell density and distribution, which caused the electrical heterogeneous of the formed cluster. Under a specific electrical stimulation, individual cells in the cell cluster may not receive the same stimulation signal and may not respond at the same time, which would lead to unsynchronized field potentials compared to stimulus signals.

The developed microfluidic device would allow to apply controlled ES to cell clusters to detect their electrical responses and perform downstream cell analysis. It will greatly facilitate the discovery of specific ES conditions to trigger desired cell cluster responses, which are critical for understanding the involved biological processes. Long-term ES (from hours to days) have been used to facilitate stem cell differentiation, which is time consuming and often required complicated device setup (Park et al. 2011; Serena et al. 2009; Yamada et al. 2007). Recently, studies have indicated that acute ES (from minutes to hours) could enhance cardiomyocytes generation from iPSCs (Hernández et al. 2016). We envision to use our device to help develop acute

ES protocols for directing cardiac cell differentiation in future studies. In the future, we plan to use the device to optimize ES conditions to facilitate the functional engineered cardiac tissue development and help define bioreactor design specifications and ES regime for improving the conductive and contractile properties of engineered cardiac tissue. We also plan to reduce the constriction channel to trap single cells and study detection circuitry with larger amplification and improved noise reduction to measure the very small FP signals from single cells.

**Acknowledgements** This work is supported by National Science Foundation of USA under award ECCS-1625544.

**Publisher's note** Springer Nature remains neutral with regard to jurisdictional claims in published maps and institutional affiliations.

## References

- S. Ahadian, J. Ramón-Azcón, S. Ostrovidov, G. Camci-Unal, V. Hosseini, H. Kaji, K. Ino, H. Shiku, A. Khademhosseini, T. Matsue, *Lab Chip* **12**, 3491 (2012)
- A. Al Abed, N.H. Lovell, G. Suaning, S. Member, S. Dokos, in *Eng. Med. Biol. Soc. (EMBC), 2015 37th Annu. Int. Conf. IEEE* (2015), pp. 2287–2290
- T.J. Blanche, *J. Neurophysiol.* **93**, 2987 (2005)
- K.F. Chambers, E.M.O. Mosaad, P.J. Russell, J.A. Clements, M.R. Doran, *PLoS One* **9**, e111029 (2014)
- Y.C. Chan, S. Ting, Y.K. Lee, K.M. Ng, J. Zhang, Z. Chen, C.W. Siu, S.K.W. Oh, H.F. Tse, *J. Cardiovasc. Transl. Res.* **6**, 989 (2013)
- W. Cheng, N. Klauke, H. Sedgwick, G.L. Smith, J.M. Cooper, *Lab Chip* **6**, 1424 (2006)
- W. Cheng, N. Klauke, G. Smith, J.M. Cooper, *Electrophoresis* **31**, 1405 (2010)

- X. Dai, W. Zhou, T. Gao, J. Liu, C.M. Lieber, *Nat. Nanotechnol.* **11**, 776 (2016)
- Z. Du, O. Bondarenko, D. Wang, M. Rouabhia, Z. Zhang, *J. Cell. Physiol.* **231**, 1301 (2016)
- G. Eng, B.W. Lee, L. Protas, M. Gagliardi, K. Brown, R.S. Kass, G. Keller, R.B. Robinson, G. Vunjak-Novakovic, *Nat. Commun.* **7**, 10312 (2016)
- D. Eytan, S. Marom, *J. Neurosci.* **26**, 8465 (2006)
- R.D. Fields, K. Itoh, *Trends Neurosci.* **19**, 473 (1996)
- U. Frey, U. Egert, F. Heer, S. Hafizovic, A. Hierlemann, *Biosens. Bioelectron.* **24**, 2191 (2009)
- F. Heer, S. Hafizovic, W. Franks, T. Ugniwenko, A. Blau, C. Ziegler, A. Hierlemann, in *Proc. ESSCIRC 2005 31st Eur. Solid-State Circuits Conf.* (2005)
- D. Hernández, R. Millard, P. Sivakumaran, R.C.B. Wong, D.E. Crombie, A.W. Hewitt, H. Liang, S.S. C. Hung, A. Pébay, R.K. Shepherd, G.J. Dusting, S.Y. Lim, in *Stem Cells Int.* (2016)
- M. Hutzler, A. Lambacher, B. Eversmann, M. Jenkner, R. Thewes, P. Fromherz, *J. Neurophysiol.* **96**, 1638 (2006)
- R. Huys, D. Braeken, D. Jans, A. Stassen, N. Collaert, J. Wouters, J. Loo, S. Severi, F. Vleugels, G. Callewaert, K. Verstreken, C. Bartic, W. Eberle, *Lab Chip* **12**, 1274 (2012)
- M. Jenkner, M. Tartagni, A. Hierlemann, R. Thewes, in *IEEE J. Solid-State Circuits* (2004)
- S. Joucla, B. Yvert, *J. Physiol. Paris* **106**, 146 (2012)
- S.B. Jun, M.R. Hynd, K.L. Smith, J.K. Song, J.N. Turner, W. Shain, S.J. Kim, *Med. Biol. Eng. Comput.* **45**, 1015 (2007)
- I.S. Kim, J.K. Song, Y.L. Zhang, T.H. Lee, T.H. Cho, Y.M. Song, D.K. Kim, S.J. Kim, S.J. Hwang, *Biochim. Biophys. Acta - Mol. Cell Res.* **1763**, 907 (2006)
- N. Klauke, G.L. Smith, J. Cooper, *Biophys. J.* **85**, 1766 (2003)
- N. Klauke, G.L. Smith, J. Cooper, *Biophys. J.* **91**, 2543 (2006)
- A. Kotwal, C.E. Schmidt, *Biomaterials* **22**, 1055 (2001)
- A. Llucià-Valldeperas, B. Sanchez, C. Soler-Botija, C. Gálvez-Montón, S. Roura, C. Prat-Vidal, I. Perea-Gil, J. Rosell-Ferrer, R. Bragos, A. Bayes-Genis, *Stem Cell Res Ther* **5**, 93 (2014)
- A. Llucià-Valldeperas, B. Sanchez, C. Soler-Botija, C. Gálvez-Montón, C. Prat-Vidal, S. Roura, J. Rosell-Ferrer, R. Bragos, A. Bayes-Genis, *J. Tissue Eng. Regen. Med.* **9**, E76 (2015)
- D. Malleo, J.T. Nevill, A. Van Ooyen, U. Schnakenberg, L.P. Lee, H. Morgan, *Rev. Sci. Instrum.* **81**, 016104 (2010)
- S. Martinoia, N. Rosso, M. Grattarola, L. Lorenzelli, B. Margesin, M. Zen, *Biosens. Bioelectron.* **16**, 1043 (2001)
- F.B. Myers, O.J. Abilez, C.K. Zarins, L.P. Lee, in *Proc. Annu. Int. Conf. IEEE Eng. Med. Biol. Soc. EMBS* (2011), pp. 4030–4033
- F.B. Myers, C.K. Zarins, O.J. Abilez, L.P. Lee, *Lab Chip* **13**, 220 (2013)
- R. Nuccitelli, *Bioelectromagnetics* **13**, 147 (1992)
- S.Y. Park, J. Park, S.H. Sim, M.G. Sung, K.S. Kim, B.H. Hong, S. Hong, *Adv. Mater.* **23**, H263 (2011)
- A. Pavesi, M. Soncini, A. Zamperone, S. Pietronave, E. Medico, A. Redaelli, M. Prat, G.B. Fiore, *Biotechnol. Bioeng.* **111**, 1452 (2014)
- M. Schuettler, M. Franke, T.B. Krueger, T. Stieglitz, *J. Neurosci. Methods* **171**, 248 (2008)
- E. Serena, E. Figallo, N. Tandon, C. Cannizzaro, S. Gerech, N. Elvassore, G. Vunjak-Novakovic, *Exp. Cell Res.* **315**, 3611 (2009)
- M.E. Spira, A. Hai, *Nat. Nanotechnol.* **8**, 83 (2013)
- A. Stett, U. Egert, E. Guenther, F. Hofmann, T. Meyer, W. Nisch, H. Haemmerle, *Anal. Bioanal. Chem.* **377**, 486 (2003)
- S.-Y. Wu, H.-S. Hou, Y.-S. Sun, J.-Y. Cheng, K.-Y. Lo, *Biomicrofluidics* **9**, 054120 (2015)
- M. Yamada, K. Tanemura, S. Okada, A. Iwanami, M. Nakamura, H. Mizuno, M. Ozawa, R. Ohyama-Goto, N. Kitamura, M. Kawano, K. Tan-Takeuchi, C. Ohtsuka, A. Miyawaki, A. Takashima, M. Ogawa, Y. Toyama, H. Okano, T. Kondo, *Stem Cells* **25**, 562 (2007)
- X. Yuan, D.E. Arkonac, P.G. Chao, G. Vunjak-Novakovic, *Sci. Rep.* **4**, 3674 (2015)
- M. Zhao, *Semin. Cell Dev. Biol.* **20**, 674 (2009)
- M. Zhao, H. Bai, E. Wang, J.V. Forrester, C.D. McCaig, *J. Cell Sci.* **117**, 397 (2003)